

The dark nature of GRB 051022 and its host galaxy[★]

A. J. Castro-Tirado¹, M. Bremer², S. McBreen³, J. Gorosabel¹, S. Guziy^{1,4}, R. M. González Delgado¹, G. Bihain^{5,6}, T. Fakhullin⁷, S. B. Pandey^{1,8}, M. Jelínek¹, A. de Ugarte Postigo¹, V. Sokolov⁷, K. Misra⁹, R. Sagar⁹, P. Bama¹⁰, A. P. Kamble¹¹, G. C. Anupama¹², J. Licandro^{4,13}, F. J. Aceituno¹, and R. Neri²

¹ Instituto de Astrofísica de Andalucía (IAA-CSIC), P.O. Box 3.004, E-18.080 Granada, Spain.

² Institute de Radioastronomie Milimetrique (IRAM), 300 rue de la Piscine, 38406 Saint Martin d'Hères, France.

³ Max-Planck-Institut für extraterrestrische Physik, 85748 Garching, Germany.

⁴ Nikolaev State University, Nikolskaya 24, 54030 Nikolaev, Ukraine.

⁵ Instituto de Astrofísica de Canarias (IAC), Via Láctea s/n, La Laguna, Tenerife, Spain.

⁶ Consejo Superior de Investigaciones Científicas (CSIC), Spain.

⁷ Special Astrophysical Observatory (SAO-RAS), Nizhniy Arkhyz, Karachai-Circassian Rep., 369167 Russia

⁸ Mullard Space Science Laboratory, University College London, Holmbury St. Mary, Dorking, Surrey, RH5 6NT, UK

⁹ Aryabhata Research Institute of Observational Sciences (ARIES), Manora Peak, Nainital 263 129, India.

¹⁰ Centre for Research and Education in Science and Technology (CREST), Indian Institute of Astrophysics Shidlaghatta Road, Hosakote 562 114, India.

¹¹ Raman Research Institute (RRI), Bangalore 560 080, India.

¹² Indian Institute of Astrophysics, Koramangala, Bangalore 560 034, India.

¹³ Isaac Newton Group of Telescopes, P.O. Box 321, E-38700 Santa Cruz de la Palma (Tenerife), Spain.

Received / Accepted

ABSTRACT

Aims. We present multiwavelength (X-ray/optical/near-infrared/millimetre) observations of GRB 051022 between 2.5 hours and ~ 1.15 yr after the event. It is the most intense gamma-ray burst ($\sim 10^{-4}$ erg cm⁻²) detected by HETE-2, with the exception of the nearby GRB 030329.

Methods. Optical and near infrared observations did not detect the afterglow despite a strong afterglow at X-ray wavelengths. Millimetre observations at Plateau de Bure (PdB) detected a source and a flare, confirming the association of this event with a moderately bright ($R = 21.5$) galaxy.

Results. Spectroscopic observations of this galaxy show strong [O II], H β and [O III] emission lines at a redshift of 0.809. The spectral energy distribution (SED) of the galaxy implies A_V (rest frame) = 1.0 and a starburst occurring ~ 25 Myr ago, during which the star-forming-rate reached $\geq 25 M_{\odot}/\text{yr}$. In conjunction with the spatial extent ($\sim 1''$) it suggests a very luminous ($M_V = -21.8$) blue compact galaxy, for which we also find with $Z \sim Z_{\odot}$. The X-ray spectrum shows evidence of considerable absorption by neutral gas with $N_{\text{H},\text{X-ray}} = 3.47^{+0.48}_{-0.47} \times 10^{22}$ cm⁻² (rest frame). Absorption by dust in the host galaxy at $z = 0.809$ certainly cannot account for the non-detection of the optical afterglow, unless the dust-to-gas ratio is quite different than that seen in our Galaxy (i.e. large dust grains).

Conclusions. It is likely that the afterglow of the dark GRB 051022 was extinguished along the line of sight by an obscured, dense star forming region in a molecular cloud within the parent host galaxy. This galaxy is different from most GRB hosts being brighter than L^* by a factor of 3. We have also derived a SFR $\sim 50 M_{\odot}/\text{yr}$ and predict that this host galaxy will be detected at sub-mm wavelengths.

Key words. gamma rays: bursts – techniques: photometric – techniques: spectroscopic – X-rays: general – cosmology: observations

1. Introduction

The first gamma-ray burst (GRB) with a fading X-ray afterglow and without an optical counterpart was detected by *BeppoSAX* in Jan 1997 (Feroci et al. 1997, Gorosabel et al. 1998). The number of similar events has continued to increase during the Afterglow Era. Dark GRBs seem to constitute a significant fraction of the

GRB population (eg Filliatre et al 2006). Although in these cases where no optical/near infrared (nIR) afterglows have been detected, transient X-ray and radio emission has pinpointed the parent galaxies where the bursts occurred. About 48% (34/71) of GRBs that were localised by *Swift*/XRT during the first year of the mission do not show an optical (or near-IR) afterglow, despite deep searches (down to ~ 21 -22 mag) performed for nearly all events within 24 hr.

Proposed explanations include obscuration, a low-density environment, intrinsic faintness and a high-redshift location (also discussed by Jakobsson et al. 2004, Rol et al. 2005, Fynbo et al. 2001). The first possibility could be due to: i) a high column density of gas around the progenitor like a dusty, clumpy medium in a giant molecular cloud (GMCs, Lamb 2001) or ii) to dust in the host galaxy at larger distances which can account for only $\sim 10\%$ of the events (discussed in Piro et al. 2002). The

Send offprint requests to: A.J. Castro-Tirado, e-mail: ajct@iaa.es

[★] Based on observations taken with the 1.0m telescope at ARIES, with the 2.0 m telescope at Hanle, with the 1.5 m Carlos Sánchez at Observatorio del Teide, with the 1.5 m telescope at Observatorio de Sierra Nevada, with the 3.5m Telescope at the Spanish-German Calar Alto Observatory, with the 3.5 m Telescopio Nazionale Galileo, with the 4.2 m William Herschel telescope, at the Observatorio del Roque de los Muchachos in La Palma, and with the 6.0 m Bolshoi Azimuthal Telescope at the Special Astrophysical Observatory in Zelenchukskaya.

occurrence of a burst in a low-density ambient medium (Taylor et al. 2000) will result in a very dim afterglow, although this seems unlikely due to the accepted association between long-duration GRBs and core-collapse supernova whose progenitors would not have had time to travel too far from their birth places in star-forming regions. The high- z case, in which the Ly- α forest emission will affect the optical band, it is only applicable for $\geq 10\%$ of the events (see Gorosabel et al. 2004).

Therefore it is essential to find new potential dark GRBs and to study whether the *darkness* is due to the obscuration scenario (the a-priori most plausible scenario for the reasons given above). Thus, the bright GRB 051022 constituted a perfect case study. It was discovered by *HETE-2* on 22 Oct 2005 (Olive et al. 2005). The burst started at 13:07 UT and lasted for ≈ 200 s, putting it in the “long-duration” class of GRBs (Tanaka et al. 2005). It was also observed by *Mars Odyssey* and *Konus/WIND* (Hurley et al. 2005). It had a fluence of $(2.20 \pm 0.02) \times 10^{-5}$ erg cm^{-2} in the 2-30 keV range and $(1.40 \pm 0.02) \times 10^{-4}$ erg cm^{-2} in the 30-400 keV energy band, making it the highest fluence event detected by *HETE-2* in its 6-yr lifetime, with the sole exception of the nearby GRB 030329 (Ricker 2005). The average spectrum of the prompt emission was best fit by an absorbed Band model with $\alpha = 1.01^{+0.02}_{-0.03}$, $\beta = 1.95^{+0.25}_{-0.14}$, $E_{\text{peak}} = 213 \pm 18$ keV with $N_{\text{H}} = (1.51^{+0.53}_{-0.50}) \times 10^{22}$ atoms cm^{-2} (Nakagawa et al. 2006). Golenetskii et al. (2005) report the best fit to the Konus data is a power law with exponential cutoff model with $\alpha = 1.176 \pm 0.038$ and $E_{\text{peak}} = 510^{+37}_{-33}$ keV in the 20 keV - 2 MeV energy range, a higher value than derived by *HETE-2*. The prompt dissemination (55.0 s) of the GRB position by *HETE-2* enabled rapid responses by automated and robotic telescopes like ROTSE-III (Schaefer et al. 2005) and ART (Torii et al. 2005), although no prompt optical afterglow was detected. *Swift* slewed and started data acquisition (about 3.5 hr after the event) and fading X-ray emission was detected by the XRT, which can be considered as the first clear detection of the afterglow from GRB051022 (Racusin et al. 2005a). This result triggered a multiwavelength campaign at many observatories aimed at detecting the afterglow at other wavelengths.

Here we report the results of the multiwavelength observations carried out, from millimetre wavelengths to the X-ray band, for both the afterglow and for the host galaxy, and we discuss the implications of the study for dark GRBs.

2. Observations and data reduction

2.1. Optical and near-IR observations

Target of opportunity (ToO) observations in the optical were started 2.9 hr after the event using the 1.0 m telescope (+CCD) at ARIES and the 2.0 m telescope (+ HFOSC camera) at Hanle (near Himalaya in India). Additional optical observations were made at 1.5 m telescope (+ CCD) at Observatorio de Sierra Nevada in Granada (Spain). Near-IR (nIR) observations were started at the 1.5 m Carlos Sánchez telescope (+ CAIN-2) at Observatorio the Izaña en Tenerife (Spain) and with the 3.5 m Telescopio Nazionale Galileo (+ NICS) at Observatorio del Roque de Los Muchachos in La Palma (Spain). Spectroscopic observations of the potential host galaxy were conducted at the 4.2m William Herschel Telescope at La Palma on 7 Nov 5, using ISIS with the blue arm centred at 4500 Å and the R300B grating (3200-5300 Å, dispersion 0.86 Å/pix) and the red arm centred at 6450 Å and the R300R grating (5300-7600 Å, dispersion 0.84 Å/pix). A second spectrum was obtained with the

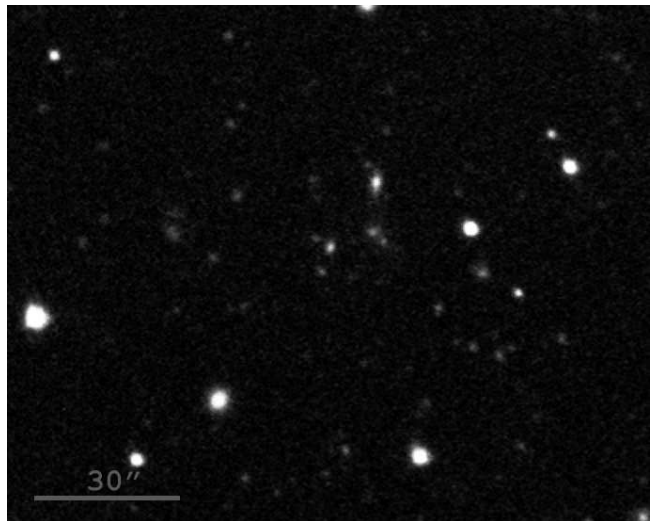


Fig. 1. The *BVR*-band composite image of the GRB 051022 field taken at the 1.5m OSN on 26 Oct 2005. The potential host galaxy is the bluest object in the field, close to the centre of the image. The field is $2'.1 \times 1'.7$ with North up and East to the left.

red arm centred at 8650 Å and the R300R grating (7500-9800 Å, dispersion 0.86 Å/pix). A third spectrum was obtained at the 6.0m Bolshoi Azimuthal Telescope in Caucasus on 12 Dec 2006, using SCORPIO with the VPHG400 holographic grism (3500-9500 Å, 15 Å resolution). The observation log is presented in Table 1.

In order to determine the magnitudes in all our optical and nIR images, we used aperture photometry with the DAOPHOT routine under IRAF¹. The potential host galaxy was revealed in the optical (Fig. 1). The optical field was calibrated using the calibration provided by Henden (2005). The nIR images were calibrated using the 2MASS Catalogue.

The spectroscopic observations were reduced under IRAF following the standard procedure to correct the frames from bias and flatfield. The spectra are also calibrated in wavelength, but not in flux.

2.2. Millimetre observations

Additional mm observations were obtained at the Plateau de Bure Interferometer (PdBI) as part of an on-going ToO programme. The PdBI observed the source on Oct 23, 24, 28 and 31, in the 5 antenna compact D configuration). The data reduction was done with the standard CLIC and MAPPING software distributed by the Grenoble GILDAS group, the flux calibration is relative to the carbon star MWC349. Amplitude and phase calibration were relative to the quasar 3C454.3. The observing log is presented in Table 2.

2.3. X-ray observations

The XRT on *Swift* began to observe GRB 051022 ~ 3.5 hours after the trigger and detected a decaying X-ray source in the *Swift*/XRT field at position RA(J2000)= $23^{\text{h}}56^{\text{m}}4.1^{\text{s}}$, Dec(J2000)= $+19^{\circ}36'25''$ (Racusin et al. 2005a). The XRT observations are in Photon Counting (PC) mode and were re-

¹ IRAF is distributed by the NOAO, which are operated by USRA, under cooperative agreement with the US NSF.

Table 1. Journal of optical and near-infrared (nIR) frames taken on the GRB 051022 field.

Date of exposure UT (mid exposure)	Telescope/ Instrument	Filtre/ Grism	Exposure Time (seconds)	Limiting Magnitude
22 Oct 05, 16:18	2.0HCT (HFOSC)	<i>R</i>	600	22.5
22 Oct 05, 17:00	2.0HCT (HFOSC)	<i>I</i>	600	21.8
22 Oct 05, 17:20	1.0ST (CCD)	<i>R</i>	900	20.8
24 Oct 05, 20:45	1.5OSN (CCD)	<i>B</i>	1 800	23.0
24 Oct 05, 22:15	1.5OSN (CCD)	<i>V</i>	720	22.5
24 Oct 05, 19:40	1.5OSN (CCD)	<i>R</i>	120	22.2
24 Oct 05, 19:43	1.5OSN (CCD)	<i>I</i>	120	21.3
26 Oct 05, 20:00	1.5OSN (CCD)	<i>U</i>	3 000	22.9
31 Oct 05, 03:30	1.5OSN (CCD)	<i>U</i>	6 000	23.4
07 Nov 05, 22:47	4.2WHT (ISIS)	R300B	5 400	–
07 Nov 05, 22:47	4.2WHT (ISIS)	R300B	1 800	–
07 Nov 05, 23:24	4.2WHT (ISIS)	R300R	3 600	–
12 Dec 06, 17:02	6.0BTA (SCORPIO)	VPHG400	7 200	–
23 Oct 05, 01:56	1.5TCS (CAIN-2)	<i>K_S</i>	1 800	18.0
23 Oct 05, 02:42	1.5TCS (CAIN-2)	<i>J</i>	1 800	19.0
23 Oct 05, 23:30	1.5TCS (CAIN-2)	<i>H</i>	1 800	18.5
24 Oct 05, 00:20	1.5TCS (CAIN-2)	<i>K_S</i>	1 800	18.0
20 Nov 05, 20:52	3.5TNG (NICS)	<i>J</i>	1 200	20.0
20 Nov 05, 21:28	3.5TNG (NICS)	<i>H</i>	1 200	19.5
14 Oct 06, 00:39	3.5CAHA (OMEGA2000)	<i>H</i>	2 400	20.0

Table 2. Journal of millimetre (mm) observations of the GRB 051022 field.

Date of 2005 UT (start time - end time)	Configuration	Flux (mJy, 1σ)	Frequency (GHz)	Beam (arcsec)	Position angle (°)
23.Oct 20:42 - 23.Oct 23:27	6Dp	1.14 ± 0.28	90.808	8.7 x 4.0	-103
		0.02 ± 1.68	217.827	8.9 x 1.7	+ 64
24.Oct 19:17 - 25.Oct 01:44	6Dp	0.08 ± 0.17	86.243	9.1 x 4.6	+ 79
		-2.42 ± 0.85	232.032	4.7 x 1.6	+ 73
28.Oct 20:44 - 29.Oct 01:28	6Dp	-0.33 ± 0.44	86.243	9.2 x 3.8	- 96
		1.81 ± 3.40	232.032	2.5 x 1.8	+ 57
30.Oct 15:27 - 30.Oct 18:20	5Dp	3.48 ± 1.05	90.229	10.7 x 3.5	- 57
01.Nov 20:44 - 01.Nov 01:28	6Dp	-0.50 ± 0.26	86.243	8.0 x 3.8	- 69
		0.55 ± 1.35	221.501	3.0 x 1.4	- 63

Table 3. GRB 051022 host galaxy optical and nIR photometry.

U	B	V	R	I	J	H	<i>K_S</i>
22.60 ± 0.20	22.61 ± 0.10	21.93 ± 0.12	21.50 ± 0.10	20.84 ± 0.12	20.36 ± 0.12	19.30 ± 0.08	18.15 ± 0.23

duced using the standard xrtpipeline (version 0.10.4) for XRT data analysis software² using the most recent calibration files. The spectral data were analysed with the XSPEC version 11.3 (Arnaud 1996).

The first two observations show evidence of mild pile up and an annular source region rather than a circular one was used in both of these cases (for a detailed discussion of PC pile up in XRT see Vaughan et al. 2006). The radius of the affected inner annulus was determined by fitting the point spread function to the data and selecting regions where the data are well fit by the point spread function. Inner annuli regions of 10 and 5 arcsec were excluded in this manner for orbit 1 and 2 respectively. The exposure map correction was used to account for the presence of bad columns close to the centre of the source image.

² <http://swift.gsfc.nasa.gov/docs/software/lheasoft/download.html>

In addition, the count rate was manually corrected for the loss of counts incurred by the use of an annular extraction region for the pile up correction.

3. Results and discussion

The afterglow was detected at X-ray and millimetre wavelengths, but not in the optical or near infrared bandpasses. The later non-detections are in agreement with the upper limits reported by ROTSE-III (Schaefer et al. 2005) and ART (Torii et al. 2005).

3.1. No optical/nIR afterglow

The *Swift*/XRT detected the X-ray afterglow for GRB 051022 (Racusin et al. 2005a), allowed us to promptly identify two objects (dubbed “A” and “B”, adopting the naming convention introduced by Castro-Tirado et al. 2005) in the surroundings of the XRT X-ray error box. Only object “B” was located inside the box while “A” was just 1.5 arcsec outside. Neither of the two objects were found to be varying in our images, in agreement with other early time reports by Nysewander et al. (2005) or Burenin et al. (2005).

In order to estimate the optical and nIR limiting magnitudes of the possible underlying transient at these wavelengths, we simulated a point source underlying in the host galaxy, making use of the PSF in nearby stars in the field in both the deep R_c and K_S -band images, and determined the limiting magnitude at which the simulated point source would be remained detected at a 3σ level by our detection software. These values, $R = 21.5$ and $K_S = 18.0$, are used hereafter.

3.2. Millimetre afterglow: flaring activity ?

In order to detect the elusive afterglow, mm observations were conducted at PdBI 33 hr after the burst. The afterglow was successfully detected, with a flux density of 1.14 ± 0.28 mJy at 90 GHz, at a position RA(J2000)= $23^{\text{h}}56^{\text{m}}04.15^{\text{s}}$, Dec(J2000)= $+19^{\circ}36'25''.1 (\pm 0''.6)$. The source was coincident, within errors, with the above-mentioned source B, which was found to be extended on images taken by Berger and Wyatt (2005). Thus, the position of the millimetre afterglow position is superimposed on a bright optical/nIR potential host galaxy. The mm afterglow faded substantially in 24 hours and the object was not detected on 24 Oct or 28 October. Another detection was obtained on 31 October (see Fig. 2), thus confirming the trend observed at 4.8 GHz (Fig. 1 of Rol et al. 2007). Such a mm reflaring at late epoch might be caused by an energy injection episode but the lack of detailed observations at other wavelengths prevents confirmation.

We also unsuccessfully searched for line emission around the 3mm wavelength and therefore “cut” the spectral information of the 90 GHz observations into large velocity bins ($100, 200 \text{ km s}^{-1}$) to check if there is a line profile (which should have a signal-to-noise ratio ≥ 3 , because the average over the whole continuum band would mix the line with noise and weaken it).

3.3. The X-ray afterglow

The X-ray light curve of GRB 051022 in the energy range 0.3 to 10 keV is shown in Fig. 3. The data is best fit by a broken power law with pre-break index, $\alpha_{X1} = 1.50 \pm 0.07$, post-break index $\alpha_{X2} = 2.47 \pm 0.40$ with a break at 216 ± 55 ks using a smoothing factor of 10. The fit is roughly consistent with the values reported by Racusin et al (2005b) who obtain a pre-break power law index of 1.33 ± 0.07 , a break at 2.9 ± 0.2 days (250 ± 17 ks) after which the power-law index changed to 3.6 ± 0.4 and the differences can likely be attributed to the availability of new software and responses. Rol et al (2007) report an earlier break time of 110_{-23}^{+21} ks based on the *Swift*/XRT and *Chandra* data.

The spectra shown in Fig. 4 were extracted individually for orbit 1, 2 and 3 to 7 and were fit simultaneously. The data have 20 counts per bin. The pre-break X-ray spectra can be fit by a photon index $\Gamma = 2.25 \pm 0.15$ and a column density of $(0.85_{-0.11}^{+0.12}) \times 10^{22} \text{ cm}^{-2}$ with $\chi^2/dof = 81/93$. A value of $3.47_{-0.47}^{+0.48} \times 10^{22}$

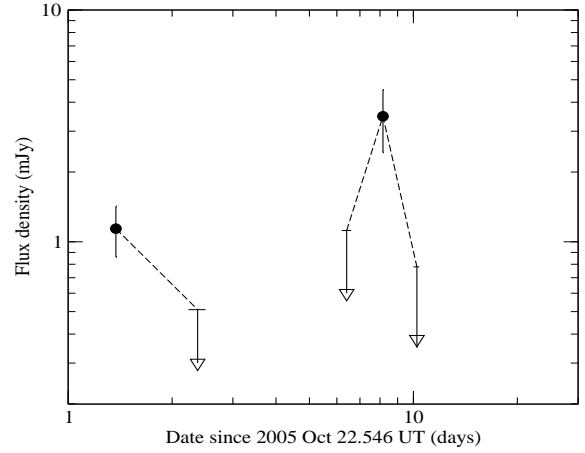


Fig. 2. The 3 mm wavelength afterglow lightcurve of GRB 051022 obtained at PdBI. Detections were obtained at 90 GHz (filled circles) whereas only upper limits were obtained at 86 GHz.

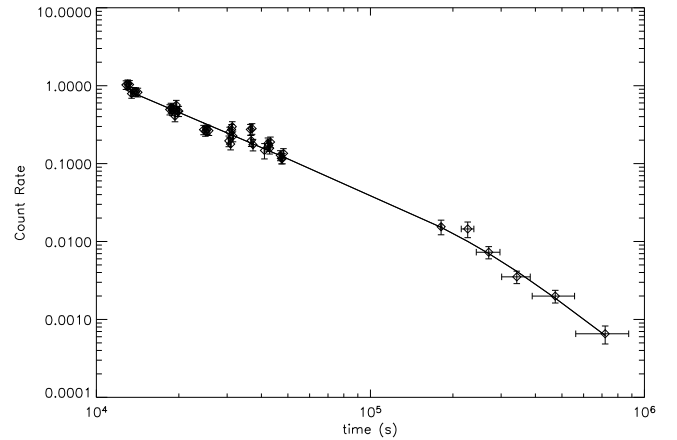


Fig. 3. The *Swift*/XRT light curve of GRB 051022. A break at $\sim 2 \times 10^5$ s is apparent on the data.

cm^{-2} was obtained for the extra absorption by a cold neutral gas within the host galaxy at redshift 0.809, in addition to the absorption within our own galaxy which is $4.09 \times 10^{20} \text{ cm}^{-2}$ (Dickey & Lockman 1990). We find no evidence for spectral evolution in the X-ray spectrum of GRB 051022. This analysis is in agreement with the XRT results obtained by Butler et al. (2005) and Rol et al. (2007). Nakagawa et al. (2006) derive a higher value of the column density of $8.8_{-1.8}^{+1.9} \times 10^{22} \text{ cm}^{-2}$ (rest frame) in the prompt emission, and Rol et al. (2007) point out that this could indicate a change in absorption between the early HETE observations and those of the XRT.

3.4. Spectral Energy Distribution modelling

We have determined the spectral energy distribution (SED) for GRB 051022 at $T_0 + 33$ hr at time of the PdBI observations (Fig 5.). The data are well fit by a jet model with $p = 2.6 \pm 0.2$, as $\alpha = (3p - 2)/4$ and $\beta = p/2$ for pre-break (isotropic emission) and $\nu_X > \nu_c$ derived from the X-ray data and assuming the slow-cooling regime (Sari et al. (1998)). We cannot distinguish whether the external medium is ISM ($\rho = \text{constant}$) or a stellar wind profile (ρ

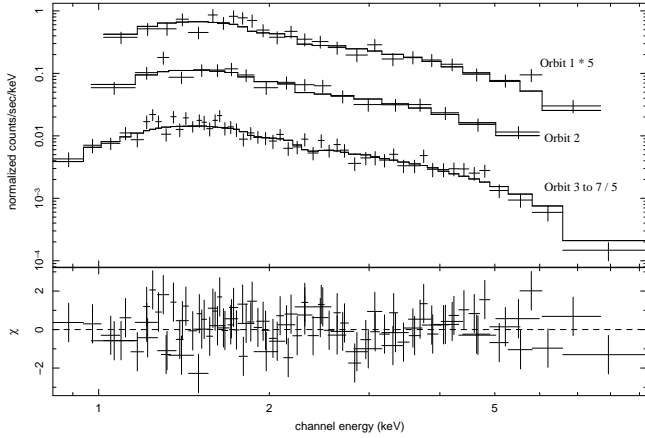


Fig. 4. Pre-break spectra of GRB 051022 including orbits 1, 2 and 3 to 7 separately. The spectra are offset as indicated for clarity of presentation.

$\propto r^{-2}$). We have also included the radio detections at the WSRT and VLA (van der Horst et al. 2005, Cameron and Frail 2005).

3.5. The obscuring medium

GRB 051022 is located undoubtedly in the dark GRB locus of the $F_{\text{opt}} - F_{\text{X-ray}}$ diagramme of Jakobsson et al. (2004). Clearly the reason that the afterglow was not detected either at optical or at nIR wavelengths is due to obscuration along the line of sight. The spectral energy distribution can be used to estimate the amount of extinction by dust at optical wavelengths and predicts a magnitude $R \sim 18.3$ at $T_0 + 33$ hr. The R band upper limit from our observations is 21.5 mag and therefore we infer a considerable extinction toward GRB 051022, with a lower limit $A_R = 3.2$ mag in the observer frame. This is equivalent to $A_V = 1.7$ mag in the rest frame at $z = 0.809$ (see next subsection) from which an equivalent Hydrogen column density at rest frame of $N_{\text{H,opt}} \geq 0.4 \times 10^{22} \text{ cm}^{-2}$ is derived, assuming the relationship $A_V = 0.56 \times N_{\text{H}} (10^{21} \text{ cm}^{-2}) + 0.23$ of Predehl & Schmitt (1995). A value of $N_{\text{H,X-ray}} = (3.47^{+0.48}_{-0.47}) \times 10^{22} \text{ cm}^{-2}$ (rest frame) was derived from the X-ray data assuming the absorbing material being in a neutral cold state. Therefore, the ratio of $N_{\text{H,X-ray}}/N_{\text{H,opt}}$ less than 9.

Comparable values of $N_{\text{H,X-ray}}$ (rest frame) were found in other GRBs like GRB 980703 (Galama & Wijers 2001) and GRB 050401 (Campana et al. 2006) and whereas substantially higher values were found in another two dark GRB host galaxies GRB 970828 (Djorgovski et al. 2001) and GRB 000210 (Piro et al. 2002), assuming the gas-to-dust ratio is compatible with the Galactic value.

Is it possible that the absorption took place in the circumburst environment of the GRB by the ISM of the host galaxy? The value of $A_V = 1.0$ derived from the host galaxy SED (see subsection 3.4) cannot account for the properties of this event assuming a dust-to-gas ratio similar to the Galactic value. Therefore the remaining possibility is that absorbing medium is a giant molecular cloud (GMC) along the line of sight and within the parent host galaxy where such high column densities would be expected. This is also supported by the high absorption column densities (within errors) derived from the *HETE-2* and *Swift*/XRT observations (see also Nakagawa et al. 2006).

3.6. The nature of the host galaxy

The optical spectrum of the GRB 051022 host galaxy (Fig. 6) shows one prominent emission line at 6731 \AA which we interpreted as [O II] 3727 \AA at a redshift $z = 0.806 \pm 0.001$. This is confirmed by the additional detection of [O III] 5007 \AA at 9071 \AA and $H\beta$ at 8806 \AA consistent with $z = 0.811$. The [O III] 4946 \AA falls within prominent sky lines and could not be accurately determined. The emission lines strengths were measured using a Gaussian fit in IRAF *splot*. No correction for underlying Balmer absorption is applied. The details are presented in Table 4. This redshift is in agreement with the value $z = 0.8$ reported by Gal-Yam et al. (2005). The corresponding luminosity distance is $D_L = 5.09 \pm 0.20 \text{ Gpc}$ (assuming $H_0 = 71 \text{ km s}^{-1} \text{ Mpc}^{-1}$, $\Omega_m = 0.27$ and $\Omega_\Lambda = 0.73$), from which Rol et al. (2007) derived a collimation-corrected energy released in gamma-rays for GRB 051022 of $(8-18) \times 10^{50} \text{ erg}$.

We derive a lower limit on the star formation rate (SFR) from the strength of the [O II] line, applying the calibration of Kennicutt (1998), $\text{SFR} (M_\odot/\text{yr}) = (1.4 \pm 0.4) \times 10^{-41} L_{[\text{OII}]}$. Using the measured line luminosity as a lower limit implies $\text{SFR} (M_\odot/\text{yr}) > 3.2 M_\odot/\text{yr}$ and the SFR becomes $\text{SFR} (M_\odot/\text{yr}) = (48 \pm 3) M_\odot/\text{yr}$ when the intrinsic $A_V = 1.0$ is taken into account.

Another independent measurement for the SFR can be obtained from the UV continuum at 2800 \AA , which is produced by massive stars in the galaxy. Using the host galaxy SED, and the Kennicutt (1998) estimator, $(M_\odot/\text{yr}) = 1.4 \times 10^{-28} L_{\nu(\text{UV})} (\text{erg s}^{-1} \text{ Hz}^{-1})$, we derive a lower limit for the $\text{SFR}(\text{UV})(M_\odot/\text{yr}) \geq 8 M_\odot/\text{yr}$, which becomes $\text{SFR}(\text{UV})(M_\odot/\text{yr}) = 59 M_\odot/\text{yr}$ when the intrinsic $A_V = 1.0$ is taken into account.

The detection of [O II] $\lambda 3727$, $H\beta$ $\lambda 4861$ and [O III] $\lambda 5007$ allowed us to estimate the value of the R_{23} metallicity indicator (Pagel et al. 1979). To calculate R_{23} we assumed a flux ratio of 1/3 of [O III] $\lambda 4959$ with respect to [O III] $\lambda 5007$. Assuming a host galaxy extinction of $A_V = 1.0$ mag, a SMC-like extinction law (Pei 1992), and correcting for the Galactic extinction ($E(B-V) = 0.06$, according to Schlegel et al. 1998) we obtained a value of $R_{23} = 4.0 \pm 0.3$. However, without detections of other emission lines (like [N II]) we can not break the R_{23} degeneracy, and there are two possible metallicity values. Given that our [O III]/[O II] flux ratio (once is corrected for Galactic and host galaxy extinction) is ~ 1 , our R_{23} yields $12+\log(\text{O}/\text{H})$ values of ~ 7.7 (lower branch) and ~ 8.7 (upper branch), respectively (see Fig. 4 of Maier et al. 2004). The metallicity-luminosity relation at medium redshift galaxies ($z = 0.64$, Maier et al. 2004) predicts a metallicity around $12+\log(\text{O}/\text{H}) \sim 9.1$ for the bright absolute magnitude of our host ($M_B = -21.8$), hence supporting the metallicity obtained with the upper R_{23} branch consistent with $Z \sim Z_\odot$.

The spectral energy distribution of the GRB 051022 host galaxy is shown in Fig. 7. The restframe colours (and therefore the associated K-corrections) have been obtained based on the HyperZ code (Bolzonella et al. 2000), fitting synthetic SED templates to our *UBVRIJK_s*-band magnitudes derived from our own data (see Table 3 and correcting all for the Galactic reddening $E(B-V) = 0.06$, Schlegel et al. 1998). At $z = 0.809$, this is a rather luminous galaxy, with $M_B = -21.8$ (or $3 \times L^*$ adopting $M_B = -20.6$ for a L^* galaxy from Schechter (1976)).

Using an apparent size of $\sim 1''$ in our images, this would correspond to about 8 kpc at $z = 0.809$, typical of compact galaxies and therefore it is possible that the GRB 051022 host would be a blue compact galaxy. Its M_B value would place it at the top of their luminosity distribution (Bergvall & Östlin 2002).

Table 4. Emission lines detected in the GRB 051022 host galaxy.

Line ID	λ_{obs}	z	Flux (10^{-16} erg cm $^{-2}$ s $^{-1}$)
[O II] λ 3727	6730.7	0.806	9.4 ± 0.3
H β λ 4861	8806.3	0.811	7.9 ± 0.6
[O III] λ 5007	9070.6	0.811	13.4 ± 0.5

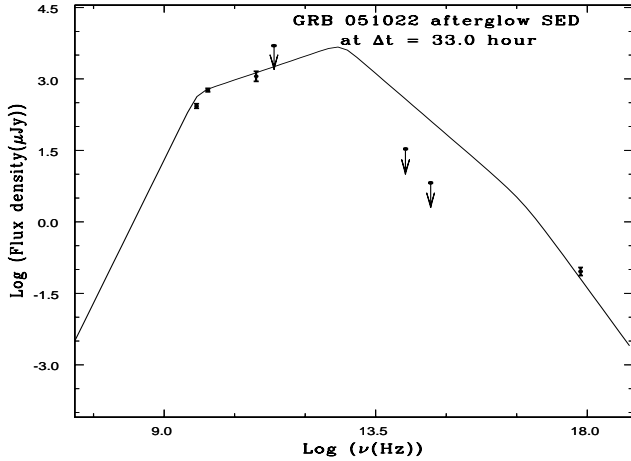


Fig. 5. The SED of the GRB 051022 afterglow at $T_0 + 33$ hr (prior to the 2.9 day break time reported by Racusin et al. (2005)). We consider $p = 2.6$, assuming the slow-cooling regime. We have also included the radio detections at the WSRT and VLA (van der Horst et al. 2005, Cameron and Frail 2005), as well as the 220 GHz and optical and near-IR upper limits reported in this paper. The initial parameters given at $T_0 + 0.06$ days are $\nu_a = 5.1 \times 10^9$ Hz, $\nu_m = 6.5 \times 10^{14}$ Hz, $\nu_c = 2.1 \times 10^{17}$ Hz and $F_{\nu,max} = 5.5$ mJy.

The mass of the GRB 051022 can be determined using several methods: i) from the fitting performed with HyperZ, we get a lower limit of $>4.3 \times 10^9 M_\odot$; ii) following Bell et al (2005), a value of $2 \times 10^{10} M_\odot$ is derived; and iii) $4 \times 10^{11} M_\odot$ from Brinchmann & Ellis (2000). The large scatter is caused by the assumptions inherent to each method.

How does the GRB 051022 host compare to other dark GRB host galaxies? Table 5 displays several properties for three dark/grey GRB host galaxies: GRB 000210 (Gorosabel et al. 2003a), GRB 000418 (Gorosabel et al. 2003b) and GRB 051022. As it can be seen, the GRB 051022 host galaxy seems to be a luminous galaxy ($M_B = -21.8$), with a SFR of $\sim 50 M_\odot/\text{yr}^{-1}$, among the highest SFR found in GRB host galaxies.

4. Conclusions

We have shown multiwavelength observations of the long duration gamma-ray burst detected by *HETE-2* (GRB 051022) between 2.5 hours and ~ 30 days after the event. Although a mm transient was found, no optical/nIR afterglow emission has been detected at the position of the X-ray afterglow detected by *Swift*.

The X-ray spectrum show evidence of absorption by neutral gas with $N_{\text{H},X\text{-ray}} = 0.85 \times 10^{22}$ cm $^{-2}$ (in the observer frame), but ISM absorption by dust in the host galaxy at $z = 0.809$ cannot fully account for the non-detection of the optical (and nIR)

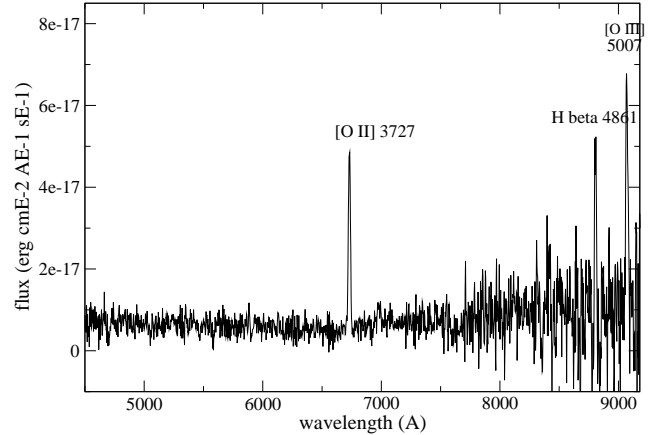


Fig. 6. The optical spectrum of the GRB 051022 host galaxy taken at the 6.0m BTA (+SCORPIO) on 12 Dec 2006. Residuals of sky emission features are visible above 7700 Å. The three emission lines detected are consistent with $z = 0.809 \pm 0.002$.

afterglow. Therefore we are left with the possibility that that the afterglow was extinguished along the line of sight by a giant Molecular cloud (GMC) where the $N_{\text{H},X\text{-ray}}$ values are typical to the one found here and therefore no optical/nIR afterglow could be detected as $A_V \sim 50$ mag ($A_K \sim 6$ mag).

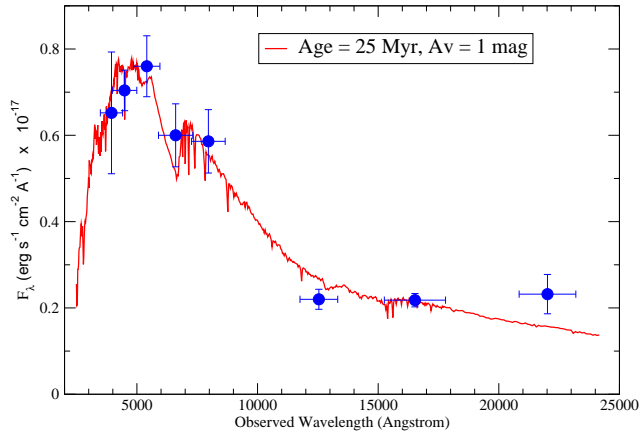
GRB 051022 is one of the most intense dark GRBs detected in the afterglow era and its host galaxy is, unlike, most of the GRB hosts, brighter than L^* . We have also shown that the host galaxy is forming stars at a significant rate and derived a SFR (UV) $\geq 8 M_\odot/\text{yr}$. We foresee that this galaxy will be detected as sub-mm wavelengths as was the case for the host galaxies of GRB 000210 and GRB 000418 (Berger et al. 2003).

The synergy between missions like *HETE-2* and *Swift*, the latter being able to be repositioned and detect the X-ray afterglow, will allow to study the population of dark GRBs to determine if extinction in the host galaxy (as we have argued in the case for GRB 051022) is the reason that about one-half of afterglows are beyond the reach of current optical telescopes.

Acknowledgements. We thank the anonymous referee for useful comments. This work is based partly on observations carried out with the IRAM Plateau de Bure Interferometer. IRAM is supported by INSU/CNRS (France), MPG (Germany) and IGN (Spain). This work has partially made use of data products from the Two Micron All Sky Survey (2MASS), which is a joint project of the Univ. of Massachusetts and the Infrared Processing and Analysis Center/California Institute of Technology, funded by the National Aeronautics and Space Administration and the National Science Foundation. This research has also been partially supported by the Ministerio de Ciencia y Tecnología under the programmes AYA2004-01515 and ESP2005-07714-C03-03 (including

Table 5. Host galaxies of dark/grey GRBs.

GRB (YYMMDD)	redshift	A_V (host) (mag)	M_B	Starburst age (Myr)	SFR (M_\odot/yr)
000210	0.842	0	-19.0	~180	2.1
000418	1.118	0.12	-20.6	~50	7.6
051022	0.809	1.0	-21.8	~25	~50

GRB 051022 host galaxy SED**Fig. 7.** The SED of the GRB 051022 host galaxy from the U to the K_S band. The data are well fit ($\chi^2/dof = 1.04$) by a Im model with considerable extinction, A_V (host) = 1.0 mag and by a starburst episode starting ~ 25 Myr ago.

FEDER funds). SMB acknowledges the support of the European Union through a Marie Curie Intra-European Fellowship within the Sixth Framework Program.

References

- Arnaud K. A., 1996, ASP Conf. Ser., 101, 17
 Bell, E. F., Papovich, C., Wolf, C. et al. 2005, ApJ 625, 23
 Berger, E., Cowie, L. L. & Kulkarni, S. R. et al. 2003, ApJ 588, 99
 Berger, E. & Wyatt, P. 2005, GCN Circ. 4148
 Bergvall, N. & Östlin, G. 2002, A&A 390, 891
 Bolzonella, M., Miralles, J.-M. & Pelló, R. 2000, A&A 363, 476
 Brinchmann, J. and Ellis, R. S. 2000, ApJ 536, 177
 Burenin, R., Denisenko, D., Pavlinsky, M. et al. 2005, GCN Circ. 4181
 Butler, N. R., Ricker, G. R., Lamb, D. Q. et al. 2005, GCN Circ. 4170
 Campana, S., Romano, P., Covino, S. et al. 2006, A&A 449, 61
 Castro-Tirado, A. J., de Ugarte Postigo, A., Bihain, G. et al. 2005, GCN Circ. 4143
 Cameron, P. and Frail, D. 2005, GCN Circ. 4154
 Dickey, J. M., & Lockman, F. J., 1990, ARA&A, 28, 215
 Djorgovski, S. G., Frail, D. A., Kulkarni, S. R. et al. 2001, ApJ 562, 654
 Feroci, M., Antonelli, L. A., Guainazzi, M. et al. 1997, A&A 332, L29
 Filliatre, P.; Covino, S.; D'Avanzo, P. et al. 2006, A&A, 448, 971
 Fynbo, J., Jensen, B. L., Gorosabel, J. et al. 2001, A&A 369, 373
 Galama, T. J. & Wijers, R. A. M. J. 2001, ApJ 549, L209
 Gal-Yam, A., Berger, E., Fox, D. B. et al. 2005, GCN Circ. 4156
 Gorosabel, J., Castro-Tirado, A. J., Wolf, C. et al. 1998, A&A 339, 719
 Gorosabel, J., Christensen, L., Hjorth, J. et al. 2003a, A&A 400, 127
 Gorosabel, J., Klose, S., Christensen, L. et al. 2003b, A&A 409, 123
 Gorosabel, J., Lund, N., Brandt, S., Westergaard, N. J., & Castro Cerón, J. M. 2004, A&A 427, 87
 Jakobsson, P., Hjorth, J., Fynbo, J. P. U. et al. 2004, ApJ 617, L21
 Henden, A. A. 2005, GCN Circ. 4184

- Hurley, K., Cline, T., Mitrofanov, I. et al. 2005, GCN Circ. 4139
 Kennicutt, R. C. 1998, ARA&A 36, 189
 Lamb, D. Q. 2001, in Gamma-ray Bursts in the Afterglow Era, ed. E. Costa, F. Frontera and J. Hjorth (Berlin, Springer), 297
 Maier, C., Meisenheimer, K., & Hippelein, H., 2004, A&A 418, 475
 Nakagawa, Y. E., Yoshida, A., Sugita, S. et al. 2006, PASJ 58, L35
 Nysewander, M., Cypriano, E., LaCluyze, A. et al. 2005, GCN Circ. 4152
 Olive, J.-F., Ricker, G., Atteia, J.-L. et al. 2005, GCN Circ. 4131
 Pagel, B. E. J., Edmunds, M. G., Blackwell, D. E., et al. 1979, MNRAS 189, 95
 Pei, Y.C., 1992, ApJ 395, 130
 Piro, L., Frail, D. A., Gorosabel, J., et al. 2002, ApJ 577, 680
 Predehl, P. & Schmitt, J. H. M. M. 1995, A&A 293, 889
 Racusin, J., Burrows, D., Gehrels, N. et al. 2005a, GCN Circ. 4141
 Racusin, J., Kennea, J., Burrows, D. et al. 2005b, GCN Circ. 4169
 Rol, E., van der Horst, A., Wiersema, K. et al. 2007, ApJ, accepted (astro-ph/0706.1518)
 Ricker, G., 2005, priv. comm
 Rol, E., Wijers, R. A. M. J., Kouveliotou, C., Kaper, L. & Kaneko, Y. 2005, ApJ, 624, 868
 Rol, E., van der Horst, A., Wiersema, K. et al. 2007, ApJ, accepted (astro-ph/0706.1518)
 Sari, R., Piran, T. & Narayan, R. 1998, ApJ 497, L17
 Schaefer, B.E. et al. 2005, GCN Circ. 4132
 Schechter, P. 1976, ApJ 203, 297
 Schlegel, D. J., Finkbeiner, D. P., & Davis, M. 1998, ApJ, 500, 525
 Tanaka, K., Ricker, G., Atteia, J.-L. et al. 2005, GCN Circ. 4137
 Taylor, G. B., Frail, D. A., Kulkarni, S. R. et al. 2000, ApJ 502, L115
 Torii, K. et al. 2005, GCN Circ. 4130
 van der Horst, A. J., Rol, E. and Wijers, R. A. M. J. 2005, GCN Circ. 4158
 Vaughan, S., Goad, M. R., Beardmore, A. P. et al., 2006, ApJ, 638, 920

List of Objects

- 'GRB 051022' on page 1
 'GRB 051022' on page 2
 'GRB 051022' on page 3
 'GRB 051022' on page 4
 'GRB 051022' on page 4
 'GRB 980703' on page 5
 'GRB 050401' on page 5
 'GRB 970828' on page 5
 'GRB 000210' on page 5
 'GRB 051022' on page 6
 'GRB 000210' on page 6
 'GRB 000418' on page 6
 'GRB 051022' on page 6